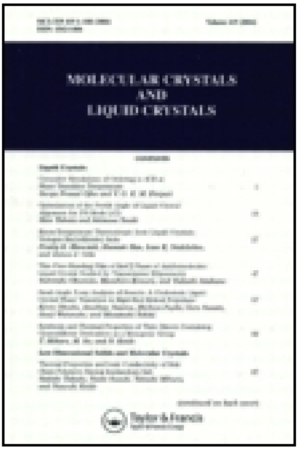

Molecular Crystals and Liquid Crystals Science and Technology. Section A. Molecular Crystals and Liquid Crystals

Publication details, including instructions for authors and subscription information:
http://www.tandfonline.com/loi/gmcl19

A Molecular Dynamics Simulation Study of Dipole Correlation in the Isotropic Phase of the Mesogens me5NF and GGP5Cl

Melanie J. Cook [a] & Mark R. Wilson [a]

[a] Department of Chemistry, University of Durham, South Road, Durham, DH1 3LE, Uk

Version of record first published: 24 Sep 2006

To cite this article: Melanie J. Cook & Mark R. Wilson (2001): A Molecular Dynamics Simulation Study of Dipole Correlation in the Isotropic Phase of the Mesogens me5NF and GGP5Cl, Molecular Crystals and Liquid Crystals Science and Technology. Section A. Molecular Crystals and Liquid Crystals, 357:1, 127-147

To link to this article: http://dx.doi.org/10.1080/10587250108028249

Mol. Cryst. Liq. Cryst., Vol. 357, pp. 127-147
Reprints available directly from the publisher
Photocopying permitted by license only

A Molecular Dynamics Simulation Study of Dipole Correlation in the Isotropic Phase of the Mesogens me5NF and GGP5Cl

MELANIE J. COOK and MARK R. WILSON*

Department of Chemistry, University of Durham, South Road, Durham DH1 3LE, UK

(Received August 10, 2000; In final form October 9, 2000)

Molecular dynamics simulations of the molecules me5NF and GGP5Cl have been undertaken to study dipole correlation in the isotropic phase. The simulations use an all-atom force field developed specifically for these molecules, together with a full treatment of the long range electrostatic interactions via an Ewald sum. me5NF exhibits a preference for anti-parallel dipole association as seen through the distance dependent correlation function $g_1(r)$. However, GGP5Cl shows no marked preference for parallel or anti-parallel dipole association. Both molecules show the presence of distinct parallel and anti-parallel dipole dimers in the liquid phase. For me5NF the dominant molecular pair configurations arise from favourable quadrupolar interactions between an unsubstituted phenyl ring and a second phenyl ring with fluorine and cyano substituents. In GGP5Cl, which has two fluorinated phenyl rings, molecules in the liquid phase show an intramolecular preference for an anti-parallel arrangement of C-F bond dipoles, which is absent in the gas phase. Kirkwood correlation factors, g_1, have been calculated from the simulations data. For me5NF, the g_1 result is in excellent agreement with existing experimental data. However, the g_1 result for GGP5Cl is in error. It is suggested that this discrepancy arises due to a failure to model correctly the dipole-induced dipole interactions that arise in this molecule.

Keywords: liquid crystals; g_1; dipole correlation; Kirkwood factor; molecular simulation; molecular dynamics; LCFF

1 INTRODUCTION

The effective mean square dipole moment μ_{eff} of a mesogen in a liquid phase is given by

$$\mu_{\text{eff}}^2 = g_1 \mu^2 \tag{1}$$

---

* Corresponding Author.

where μ^2 is the mean squared dipole for an isolated molecule. Here, the Kirkwood correlation factor g_1 determines the preference for local parallel or anti-parallel dipole association in the isotropic liquid. Mesogens with longitudinal dipole moments and Kirkwood factors greater than 1 have an enhanced effective dipole moment along the molecular long axis. This is desirable in mesogens designed for twisted nematic displays, as it lowers the threshold voltage for electro-optic switching.

Small changes in molecular structure often give rise to large changes in the bulk properties of liquid crystals. This is particularly true for g_1 values. For example, the two molecules 4-(*trans*-4-n-pentylcyclohexyl)benzonitrile (PCH5) and 4-(*trans*-4-n-pentylcyclohexyl)chlorobenzene (PCH5-Cl), vary only in the dipolar functional group attached to the phenyl ring. However, in the isotropic phase, close to the nematic phase transition, PCH5 favours anti-parallel dipole association ($g_1 = 0.88$) and PCH5-Cl favours parallel dipole association ($g_1 = 1.20$).

Molecular simulation is becoming a powerful tool for studying the behaviour of liquid crystal molecules [1–8]. In a recent simulation study [9], PCH5 and PCH5-Cl were investigated by classical molecular dynamics. This work showed that it is possible to predict successfully the different dipole association behaviour for the two molecules. In this case, molecular dynamics also provided a way of studying the correlation between individual parts of the mesogenic molecules. For PCH5 and PCH5-Cl this allowed the determination of which interactions were responsible for stabilizing individual pair configurations that give rise to the differences in dipole correlation observed experimentally.

In the current work we use the techniques developed in reference [9], to study two additional mesogens me5NF and GGP5Cl (figure 1). Molecular dynamics simulations are carried out in the *isotropic phase* using state-of-the-art atomistic methods, employing the all-atom (LCFF) force field developed in the preceding paper in this issue [10]. Using this methodology we calculate the distance dependent dipole correlation function $g_1(r)$ and carry out a detailed analysis of the molecular dynamics trajectories to assess which molecular pair configurations are most important in the liquid phase.

The outline of this paper is as follows. Section 2 describes the simulation methodology, section 3 presents molecular dynamics data for dipole correlation in the two mesogens me5NF and GGP5Cl and general conclusions are presented in section 4.

2 MOLECULAR DYNAMICS SIMULATIONS

For the two systems, me5NF and GGP5Cl, an initial molecular configuration was generated from a *bcc* lattice in which 216 molecules were given small ran-

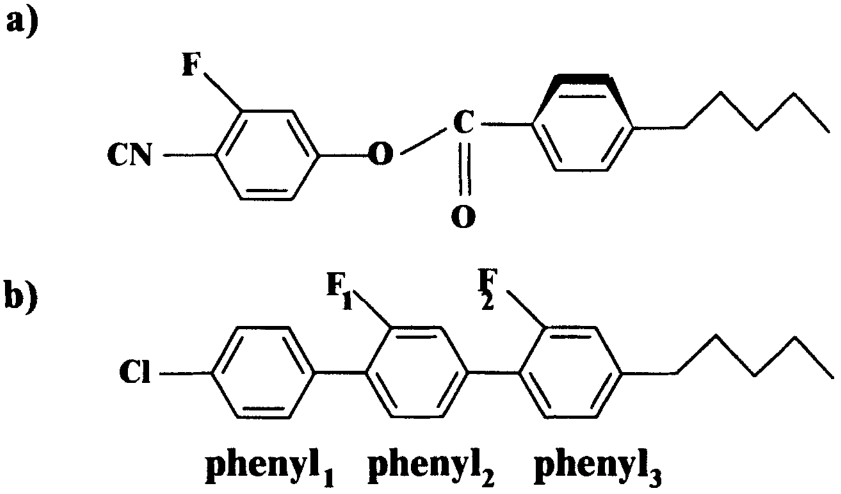

FIGURE 1 Structure of a) me5NF and b) GGP5Cl

dom displacements from their lattice positions and randomly orientated inside a cuboidal simulation box at gas phase densities. We used the all-atom (LCFF) force field described in the preceding paper [10] for all simulations. Initially, the isothermal-isobaric algorithm of Berendsen was employed to relax the molecular configuration. A nominal pressure of 10^5 Pa was used until the desired volume of approximately $6.40\text{x}10^4$Å^3 had been achieved. Thereafter the system was equilibrated using a Nosé-Hoover thermostat and a Hoover barostat at a pressure of 1 atmosphere, employing relaxation times of 1 ps and 4 ps respectively. The simulations retained cubic periodic boundary conditions throughout employing the Verlet leap frog algorithm with a time-step of 2 fs. The SHAKE procedure [11] was employed to constrain bond lengths. However, other than this molecules were treated as fully flexible, allowing for angle bending and dihedral angle changes. The *long-range* electrostatic interactions were handled by a Ewald sum with the convergence parameter α set at 0.48 Å^{-1} and 6 k-vectors were used for each of the directions (x,y,z) in the periodic box. A cut-off of 9 Å was used for the *short range* 12:6 interactions. All calculations used the DL_POLY_2.11 program [12].

For both mesogens the dipole vectors were calculated using the classical definition of μ, obtained from the molecular partial charges in the force field

$$\boldsymbol{\mu} = \sum_i q_i \mathbf{r}_i, \qquad (2)$$

which gives the direction of the dipole vector as $\hat{\boldsymbol{\mu}} = \boldsymbol{\mu}/|\mu|$.

Values of the system density ρ were monitored throughout the simulations along with values of the Kirkwood correlation factor, g_1 (equation 3) and values of the orientational correlation factor, g_2 (equation 4). In calculations of both g_1 and g_2 we used the angles between $\hat{\boldsymbol{\mu}}$, to determine θ_{ij}.

$$g_1 = 1 + \frac{1}{N}\left\langle \sum_{i}^{N}\sum_{j\neq i}^{N} \cos\theta_{ij} \right\rangle \tag{3}$$

$$\begin{aligned} g_2 &= 1 + \frac{1}{N}\left\langle \sum_{i}^{N}\sum_{j\neq i}^{N} P_2(\cos\theta_{ij}) \right\rangle \\ &= 1 + \frac{1}{N}\left\langle \sum_{i}^{N}\sum_{j\neq i}^{N} \frac{3}{2}\cos^2\theta_{ij} - \frac{1}{2} \right\rangle . \end{aligned} \tag{4}$$

Experimental dielectric and index of refraction measurements have already yielded data for g_1 in the pretransitional region at 303 K for Me5NF and 393 K for GGP5Cl. (For GGP5Cl the nematic-isotropic clearing point is at 386.8 K and Me5NF undergoes a monotropic transition to a nematic state at 296.8 K.) Simulations of the mesogens me5NF and GGP5Cl were therefore carried out at 303 K and 393 K respectively. Full equilibration of the system density required approximately 200 ps for each system. Single particle properties such as g_1 and g_2 were seen to fluctuate rapidly during the early stages of the simulation where the densities were low and molecular reorientation was rapid. After the equilibrated density was reached a further period of 500 ps was allowed for these quantities to converge to their equilibrium values. Finally, results were calculated over a further 300 ps production run. To our knowledge, these are the most extensive all-atom simulations of liquid crystal systems that have employed a proper treatment of the long range electrostatic interactions.

3 RESULTS AND DISCUSSION

3.1 Dipole and orientational correlation

A useful monitor of how dipolar and orientational correlation varies as a function of molecular separation is provided by the distance dependant correlation functions

$$g_l(r) = \langle P_l \cos(\theta_{ij}) \rangle_{\text{shell}}, \quad l = 1,2. \tag{5}$$

Here, $\langle\rangle_{\text{shell}}$ indicates an ensemble average over molecules *j* in a spherical shell of width *dr* at a distance *r* between the centres of the dipole vectors of molecules *i* and *j*.

Graphs of $g_1(r)$ are plotted in figure 2 for me5NF and GGP5Cl. Positive values indicate a preferred parallel alignment of dipoles at a distance *r* and negative values indicate a preferred anti-parallel alignment. me5NF exhibits a strong preference for anti-parallel association, as seen by the large trough in $g_1(r)$ at 3.3 Å. This trough arises from nearest neighbour interactions and has an onset of 3 Å (corresponding to the closest separation expected for two side-by-side mesogens) and extends to approximately 6 Å. Beyond 6 Å we see a small positive peak in $g_1(r)$ that arises from next nearest neighbour interactions. However, this is much smaller than the trough (at 3.3 Å) and indicates that in addition to transient dimers of aligned molecules within the liquid, we would expect to see some head-to-tail paired trimers as indicated schematically in figure 3. This is entirely consistent with the expected picture for a mesogen in the isotropic phase, where depolarized light scattering measurements indicate that short range orientational correlation arises [13], and this increases as the phase transition to a nematic phase is approached. In contrast, for GGP5Cl the $g_1(r)$ signal arising from first nearest neighbour interactions is small and positive in sign indicating a preference for local parallel dipole association. The onset of this peak is 3.5 Å and it extends to 3.8 Å. We also see a small trough from 3.8 Å to 5.9 Å, which could indicate second nearest neighbour molecules, but is more likely (as discussed below in section 3.2) to arise from nearest neighbour molecules with anti-parallel dipoles which dominate at these slightly longer distances. Finally, a small peak in $g_1(r)$ can be seen beyond 5.9 Å that most probably arises from second nearest neighbour molecules. This is indicative of the presence of small transient clusters of three aligned molecules as seen in me5NF, but in this case there is a slight preference for parallel alignment of dipoles within these clusters. The mean box lengths for me5NF and GGP5Cl are 45.99 Å and 49.37 Å respectively. In the case of both molecules, we note that $g_1(r)$ decays to zero well within half the dimensions of the cubic simulation box.

$g_2(r)$ graphs for me5NF and GGP5Cl are plotted in figure 4. The peaks centred at 3.5–3.6 Å and 5.8–5.9 Å correspond to pair and triplet interactions for aligned particles, as already indicated in the analysis of the $g_1(r)$ results. The triplet peak for GGP5Cl is rather larger than that seen for me5NF indicating that there are likely to be more transcient trimers for this material. However, we note that the corresponding peak in $g_1(r)$ at this distance is smaller. It is already known from figure 2 that me5NF shows extremely strong anti-parallel association and because of this most of the trimers will be of the form shown in figure 3. Consequently, this suggests that many of the transcient trimers for GGP5Cl are likely to

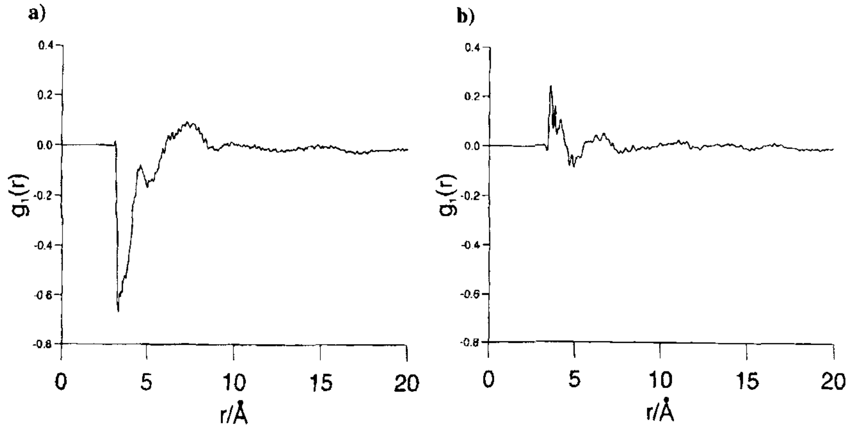

FIGURE 2 Dipolar pair correlation functions $g_1(r)$, a) me5NF at 303 K and b) GGP5Cl at 393 K

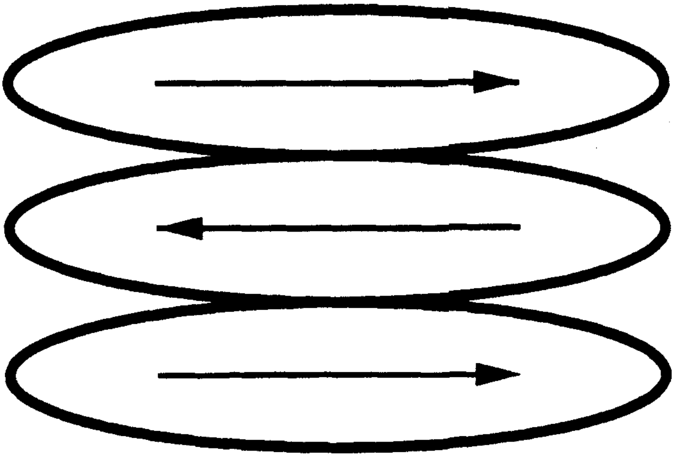

FIGURE 3 Schematic diagram showing local packing in the isotropic phase of me5NF

contain a mixture of anti-parallel and parallel associated molecules. A preference for purely parallel associated trimers would have resulted in the secondary peak in $g_1(r)$ at 5.9 Å being larger than the corresponding peak for me5NF.

$g_2(r)$ tends to zero at long distances for both materials as expected in an isotropic fluid. For PCH5 and PCH5-Cl [9], fluctuations in orientational order remained for distances equivalent to half the box length. We note that for me5NF and GGP5Cl molecules the larger system size of 216 molecules (compared to

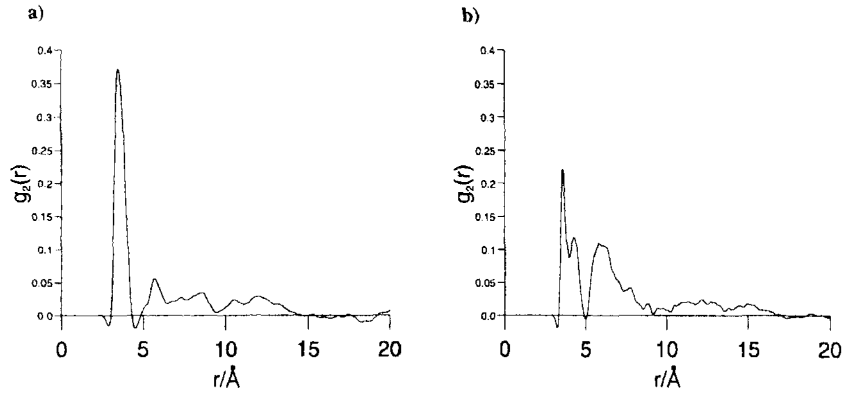

FIGURE 4 Orientational pair correlation functions $g_2(r)$, a) me5NF at 303 K and b) GGP5Cl at 393 K

125 for the cyano materials of reference [9]), seems to be sufficient for these fluctuations to die out well within half the simulation box dimensions. To check this we also calculated the system order parameter $S_2 = \langle P_2\ (\cos\theta\ )\rangle$ obtained from the largest eigenvalue obtained through diagonalising the ordering tensor

$$Q_{\alpha\beta} = \frac{1}{N}\sum_{j=1}^{N}\frac{3}{2}u_{j\alpha}u_{j\beta} - \frac{1}{2}\delta_{\alpha\beta}, \quad \alpha, \beta = x, y, z. \tag{6}$$

Here, we make use of the long axis vector $\mathbf{u}_j$ obtained through diagonalization of the moment of inertia tensor [2]

$$I_{\alpha\beta} = \sum_i m_i(s_i^2\delta_{\alpha\beta} - s_{i\alpha}s_{i\beta}), \tag{7}$$

where the atomic distance vectors $\mathbf{s}_i$ were measured relative to the molecular centre of mass. The calculated order parameters for each simulation, given in table I, are typical of those usually obtained in the isotropic phase for similar sized systems of single-site potentials (hard-spherocylinders and Gay-Berne fluids). The non-zero values are indicative of finite size effects.

TABLE I Pairwise correlation factors g_1 and g_2 for me5NF and GGP5Cl

molecule	*T/K*	g_I	g_2	$g_I(exp)$	$\langle S_2\rangle$
me5NF	303	0.79±0.005	1.55±0.017	0.78	0.0852
GGP5Cl	393	1.04±0.014	1.62±0.010	0.79	0.1064

The values of g_1 and g_2 calculated from equations 3 and 4 are given in table I. The g_1 result for the mesogen me5NF is in excellent agreement with the value obtained from experimental dielectric measurements [14] and confirms that individual molecules have a preference for anti-parallel dipole association in the isotropic phase. However, for GGP5Cl the experimental result is not reproduced. Part of the discrepancy between the experimental and calculated results may he caused by errors induced by the relatively small system size. However, the main source of error appears to arise from a subtle failure in the force field we have used. A detailed analysis of pair configurations (presented in section 3.2 below) indicates that a series of both parallel and anti-parallel dipole pair configurations arise for GGP5Cl, and that the structure of these preferred configurations are dominated by the charge distribution of the molecule. Our force field does not correctly favour the anti-parallel configurations sufficiently. The likely problem is caused by the combination of both highly polar groups and highly polarizable groups in GGP5Cl. In such circumstances we expect polarization effects to be important. The neglect of such interactions in the force field we have used (and the majority of standard molecular mechanics force fields) makes it difficult to correctly model the relative stability of pairwise associated molecules in GGP5Cl.

The g_2 values obtained for both materials are small and typical of those seen in the isotropic phase (see for example those obtained in simulation studies of hard spherocylinders in the [15]). Values of g_2 usually increase as the isotropic-nematic is approached, and can reach values of $g_2 \approx 100$ at temperatures very close to the isotropic-nematic phase transition [16].

3.2 Correlation between molecular groups

Following our previous study for PCH5 and PCH5-Cl [9], it is possible to look in detail at correlation between individual molecular groups in the two molecules within the fluid. We do this by defining a two dimensional distribution function $g(r, \pm|z|)$ [9]

$$\begin{aligned} &\text{for } \mathbf{r}_i \cdot \mathbf{r}_j \geq 0, \quad g(r,+|z|) = \frac{V}{N^2}\left\langle \sum_i \sum_{j \neq i} \delta(\mathbf{r}-\mathbf{r}_{ij})\delta(z-|z_{ij}|) \right\rangle, \\ &\text{for } \mathbf{r}_i \cdot \mathbf{r}_j \leq 0, \quad g(r,-|z|) = \frac{V}{N^2}\left\langle \sum_i \sum_{j \neq i} \delta(\mathbf{r}-\mathbf{r}_{ij})\delta(z+|z_{ij}|) \right\rangle, \end{aligned} \tag{8}$$

where $\mathbf{r}_i$, $\mathbf{r}_j$ are the axis vectors of the groups used in each molecule, $r_{ij} = |\mathbf{r}_i - \mathbf{r}_j|$ is the distance of separation between the centres of the two groups and the distances $|z_{ij}|$ are the absolute values of the projection of $\mathbf{r}_{ij}$ onto the axis vector of each molecular group (as shown in figure 5 for the molecule me5NF).

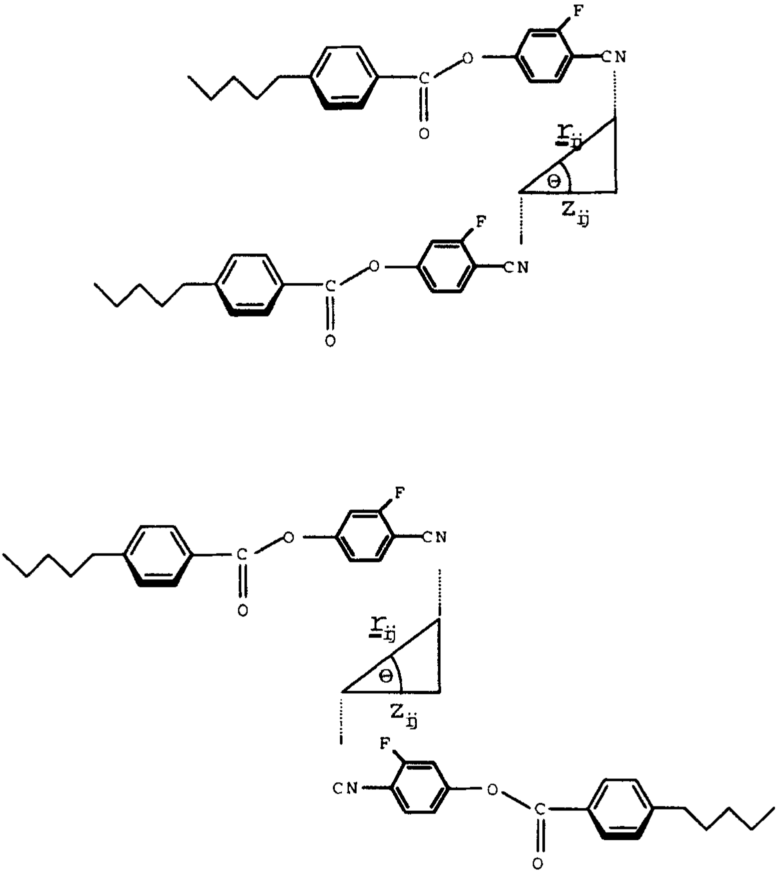

FIGURE 5 Schematic diagram showing the definition of the inter-group distances r and z for the two dimensional pair correlation functions $g(r, \pm|z|)$

As defined in equation 8, we compile two separate functions $g(r, \pm|z|)$ depending on the angles between the axis vectors of molecules i and j. Positive values $(+|z|)$ represent parallel alignment at $\mathbf{r}_i \cdot \mathbf{r}_j \geq 0$ and negative values $(-|z|)$ represent anti-parallel alignment at $\mathbf{r}_i \cdot \mathbf{r}_j \leq 0$. However, these can be represented on a single plot. We consider the positional correlation between all the main structural groups in the two mesogens me5NF and GGP5Cl, including the dipolar groups which are shown in figure 1. This generates the 15 two dimensional distribution functions for the molecule me5NF that are shown in figure 6, and the 21 two dimensional distribution functions for molecule GGP5Cl that are shown in figure 7.

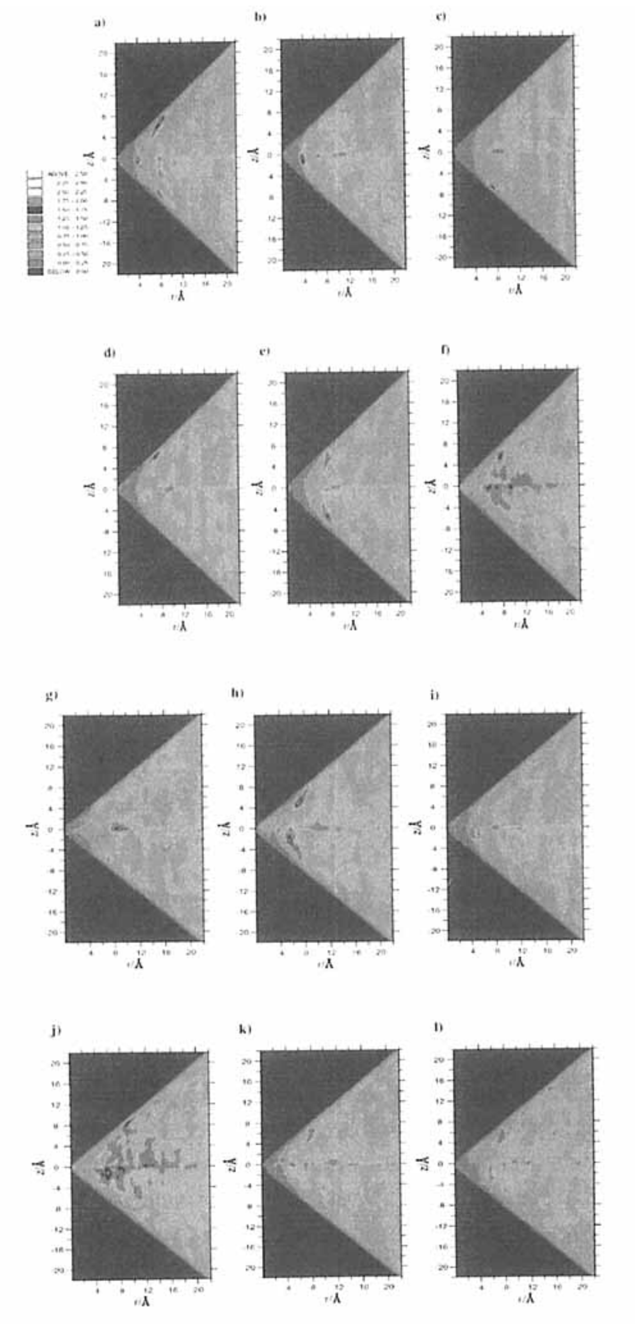
a)
b)
c)
d)
e)
f)
g)
h)
i)
j)
k)
l)
z/Å
r/Å
20
16
12
8
4
0
-4
-8
-12
-16
-20
ABOVE
BELOW

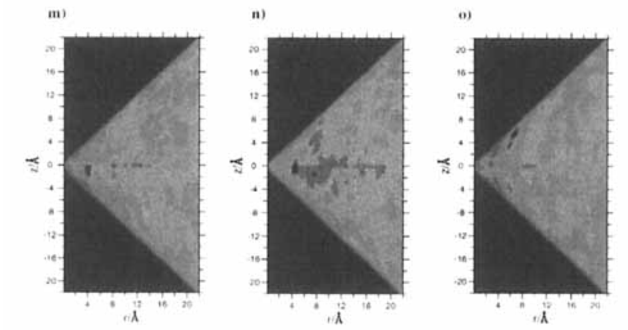

FIGURE 6 Two-dimensional correlation functions *g*(*r*, ±|*z*|) for individual groups in molecule me5NF at T=303 K. (a) C-CN-C-CN, (b) C-F-C-F, (c) ester-ester, (d) phenyl$_1$-phenyl$_1$, (e) phenyl$_2$-phenyl$_2$, (f) phenyl$_1$-phenyl$_2$, (g) C-CN-C-F, (h) C-CN-ester, (i) C-CN-phenyl$_1$, (j) C-CN-phenyl$_2$, (k) ester-phenyl$_1$, (l) ester-phenyl$_2$, (m) C-F-ester, (n) C-F-phenyl$_1$, (o) C-F-phenyl$_2$ (See Color Plate III at the back of this issue)

A number of features are immediately clear from figures 6 and 7. The series of peaks seen in the functions *g*(*r*, +|*z*|) and *g*(*r*, -|*z*|) can only be explained by the presence of both anti-parallel and parallel dipole dimers for the two molecules. There are also secondary peaks in *g*(*r*, ±|*z*|) that arise at large *r* and can only be explained by the presence of trimers (as indicated earlier in the behaviour of $g_1(r)$ and $g_2(r)$). The position of the main peaks in *g*(*r*, ±|*z*|) from figures 6 and 7 are classified in tables II and III. From the known molecular dimensions, the peaks in *g*(*r*, ±|*z*|) can be assigned to appoximate pair configurations. The major configurations are sketched in figure 8 for the me5NF and in figure 9 for the mesogen GGP5Cl and the assignment of peaks is carried out in column four of tables II and III. In figure 9 we have drawn the fluorines on opposite sides of the GGP5Cl molecule. However, we know that there is a mixture of the two fluorine conformations that arise from rotation about the phenyl$_2$-phenyl$_3$ dihedral angle (this is considered in detail below). In me5NF the most favoured pair configurations are B and D indicating both parallel and anti-parallel dipole dimers. The regions of high probability density for me5NF result mainly from strong electrostatic interactions involving the cyano groups and the phenyl rings. In configurations B and D we note the favourable quadrupolar interactions that arise from having phenyl$_1$ directly above phenyl$_2$. For a bare phenyl ring the component of the quadrupole moment perpendicular to the plane of the rings has a negative sign and consequently the centres of two parallel phenyl rings prefer to be shifted with respect to each other, rather than to be stacked directly on top of each other. (Alternatively, they prefer a herringbone packing, as in the crystal structure of

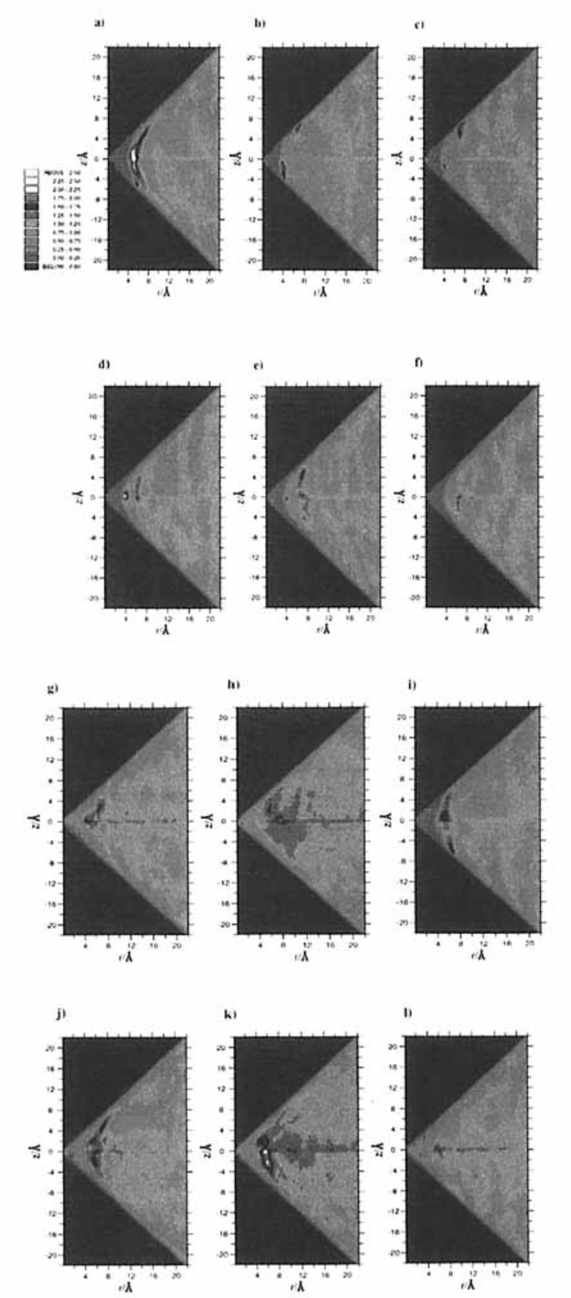
a)
b)
c)
d)
e)
f)
g)
h)
i)
j)
k)
l)
z/Å
r/Å
20
16
12
8
4
0
-4
-8
-12
-16
-20
4
8
12
16
20
ABOVE 2.50
2.25 - 2.50
2.00 - 2.25
1.75 - 2.00
1.50 - 1.75
1.25 - 1.50
1.00 - 1.25
0.75 - 1.00
0.50 - 0.75
0.25 - 0.50
0.00 - 0.25
BELOW 0.00

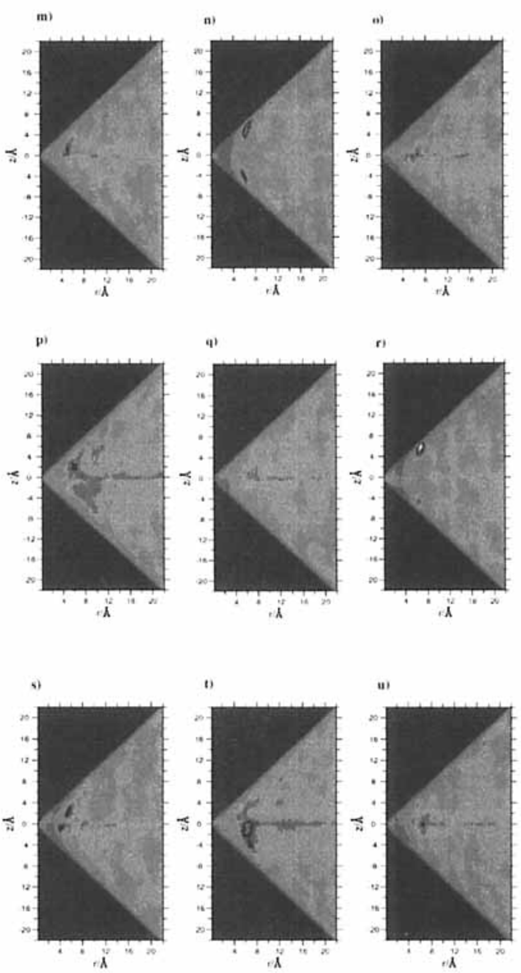

FIGURE 7 Two-dimensional correlation functions $g(r, \pm|z|)$ for individual groups in molecule GGP5Cl at T=393 K. (a) C-Cl-C-Cl, (b) C-F_1-C-F_1, (c) C-F_2-C-F_2, (d) $phenyl_1$-$phenyl_1$, (e) $phenyl_2$-$phenyl_2$, (f) $phenyl_3$-$phenyl_3$, (g) C-Cl-C-F_1, (h) C-Cl-C-F_2, (i) C-Cl-$phenyl_1$, (j) C-Cl-$phenyl_2$, (k) C-Cl-$phenyl_3$, (l) C-F_1-C-F_2, (m) C-F_1-$phenyl_1$, (n) C-F_1-$phenyl_2$, (o) C-F_1-$phenyl_3$, (p) C-F_2-$phenyl_1$, (q) C-F_2-$phenyl_2$, (r) C-F_2-$phenyl_3$, (s) $phenyl_1$-$phenyl_2$, (t) $phenyl_1$-$phenyl_3$, (u) $phenyl_2$-$phenyl_3$ (See Color Plate IV at the back of this issue)

benzene.) However, the attachment of a fluorine and a cyano group to a phenyl ring changes the sign of the quadrupole moment perpendicular to the plane of the rings. Consequently, the quadrupolar interactions favour the parallel stacking of $phenyl_1$ and $phenyl_2$ directly above each other.

TABLE II Approximate positions of the main peaks in the two dimensional translational correlation function $g(r, \pm|z|)$ for me5NF at 303 K. Positive values of z indicate parallel association and negative values of z indicate anti-parallel association. Column four indicates the pair configuration(s) from figure 8 which are responsible for each peak. ("Secondary" indicates a peak that arises from next nearest neighbour interactions or beyond.)

group interactions	*r/Å*	*z/Å*	*configurations*
C-CN-C-CN	4	0	A (strong correlation)
	8	0	A (secondary, weak)
	8	7	B (strong correlation)
C-F-C-F	4	0	A (strong correlation)
	6.5	0	A (secondary, weak)
ester-ester	7–10	0	A (secondary, weak)
	8	–7	E
phenyl$_1$-phenyl$_1$	7	6.5	B (strong correlation)
phenyl$_2$-phenyl$_2$	8.5	0	A (secondary, weak)
	7	5–6	B (weak)
	7	–6	D
phenyl$_1$-phenyl$_2$	5–6	0	B, D
	9.5	0	B, D (secondary)
	8	6	A
C-CN-C-F	9	0	A (secondary)
C-CN-ester	4	–2	E (strong correlation)
	9–12	0	B, C (secondary, weak)
	7–8	5–6.5	B (strong correlation)
C-CN-phenyl$_1$	4	–1	E (weak)
	8	0	B (secondary, weak)
C-CN-phenyl$_2$	4	–1	D (strong correlation)
	8	0	D (secondary)
	12	0	D (secondary)
ester-phenyl$_1$	5	0	C (weak)
	7	0	C (secondary, weak)
	11	0	C (secondary, weak)
	8	5	A (weak)
ester-phenyl$_2$	5	–3	D (weak)
	7.5	6.5	B
C-F-ester	4	–1	C (strong correlation)
	9	0	B, C (secondary, weak)
	12	0	B, C (secondary weak)
C-F-phenyl$_1$	8–10	0	A (secondary, weak)
	8	4–6	B
	8	–2	C
	4.5	–0.5	E
C-F-phenyl$_2$	7	5.5	B
	6	–4	C (weak)
	8.5	0	B (secondary, weak)

TABLE III Approximate positions of the main peaks in the two dimensional translational correlation function $g(r, \pm|z|)$ for GGP5Cl at 393 K. Positive values of z indicate parallel association and negative values of z indicate anti-parallel association. Column four indicates the pair configuration(s) from figure 9 which are responsible for each peak. ("Secondary" indicates a peak that arises from next nearest neighbour interactions or beyond.)

group interactions	*r/Å*	*z/Å*	*configurations*
C-Cl-C-Cl	5	−2-2	C, H (strong correlation)
C-F$_1$-C-F$_1$	4.5	−2	F
	7	6	A
C-F$_2$-C-F$_2$	4.5	−2	I
	7	6	A
phenyl$_1$-phenyl$_1$	4	0	C, E (strong correlation)
	7	0	C, E (secondary)
phenyl$_2$-phenyl$_2$	4	0	C
	8	0	C (secondary)
	7	5	A
phenyl$_3$-phenyl$_3$	7	−2-0	I
C-Cl-C-F$_1$	5	0	A, E
	6	3	B
C-Cl-C-F$_2$	6–10	0	(secondary)
	5.5	2	D
C-Cl-phenyl$_1$	6	0–2	C
	7	−6	E
C-Cl-phenyl$_2$	6	−3-0	H
	6	2	B
	7.5	5.5	A
C-Cl-phenyl$_3$	5.5	0	F (strong correlation)
	10	0	(secondary)
	6	−3	G (strong correlation)
	5.5	2	D
C-F$_1$-C-F$_2$	5.5	0	B
C-F$_1$-phenyl$_1$	4.5	1	A
	10	0	(secondary, weak)
C-F$_1$-phenyl$_2$	7	5	A
	7	−4	E
C-F$_1$-phenyl$_3$	4.5–7.5	0	B (weak)
C-F$_2$-phenyl$_1$	6	2	D
C-F$_2$-phenyl$_2$	7	0	(secondary)
C-F$_2$-phenyl$_3$	7	6	A (strong correlation)
	6.5	−5	G (weak)
phenyl$_1$-phenyl$_2$	4	−1	F
	8.5	0	(secondary, weak)
	6	2	A
phenyl$_1$-phenyl$_3$	6.5	−2-0	F, G
phenyl$_2$-phenyl$_3$	7	0	(secondary)

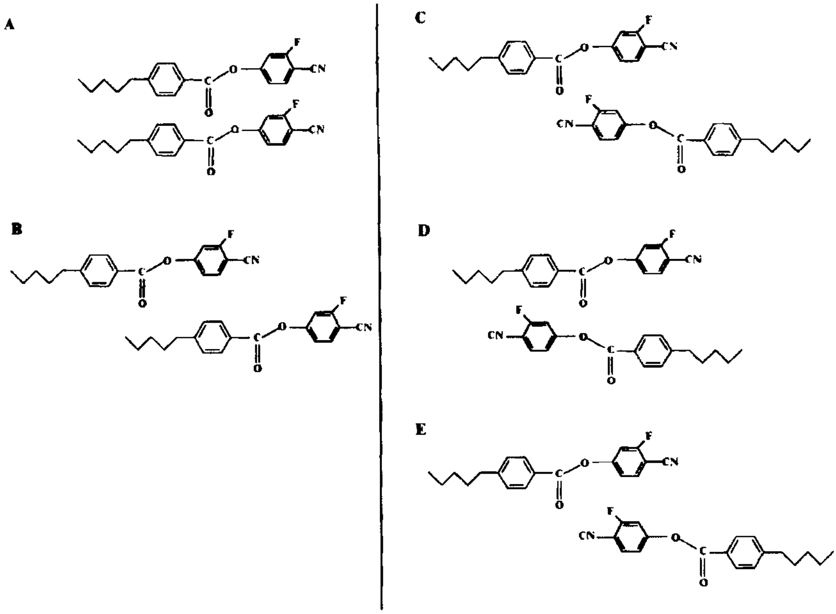

FIGURE 8 Schematic diagram showing the favoured molecular pair configurations for the mesogen me5NF

In GGP5Cl, none of the favoured pair configurations shown in figure 9 are particularly dominant. This is most probably due to the absence of a single dominant electrostatic interaction (such as the phenyl$_1$-phenyl$_2$ quadrupole interaction in me5NF). Instead, a range of electrostatically favoured configurations are possible: parallel stacked fluorinated rings with the centre of one ring shifted slightly relative to the centre of the other ring, or stacked rings with the fluorines on opposite sides.

We note that the picture of dipole correlation presented in this work is consistent with the theory of pairwise association of Dunmur and Toriyama [17]. The latter considers an equilibrium between parallel and anti-parallel dipole species and works well for dilute solutions of mesogens where there is molecular association to form transient dimers. However, in the liquid phase the situation is rather more complicated with evidence for several transient parallel and anti-parallel dimers, as well as some transient trimer species. Experimental dielectric measurements also provide strong evidence for coincident parallel and anti-parallel dipole association. Dunmur and Toriyama have presented experimental measurements for mesogens in solutions of isotropic [17,18] or liquid crystalline solvents [19] that can be interpreted in terms of the pairwise association model.

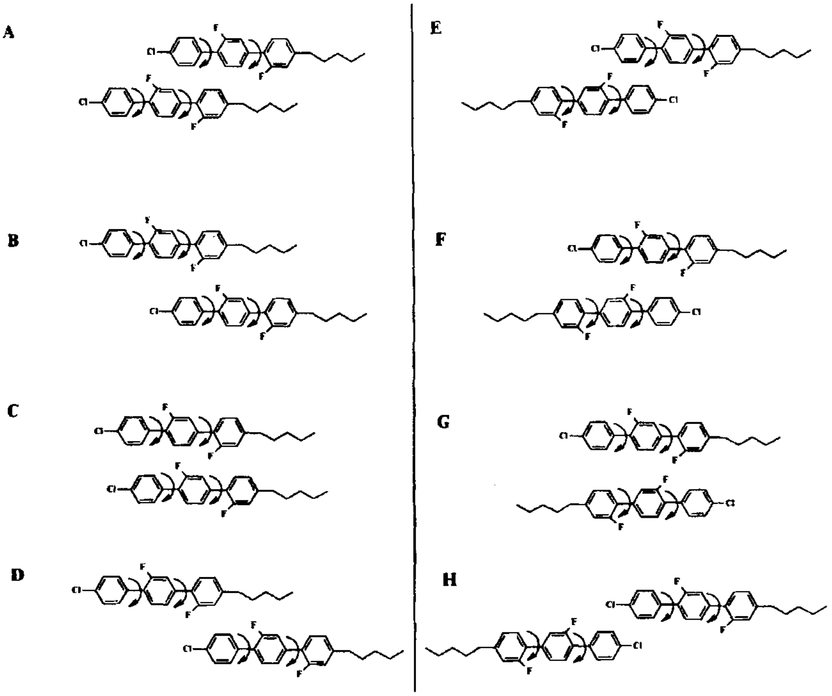

FIGURE 9 Schematic diagram showing the favoured molecular pair configurations for the mesogen GGP5Cl. Arrows indicate that the configurations shown correspond to an average of the conformations that arise from rotation about the inter-ring torsional angles

It is interesting to consider how the fluorines in the core of GGP5Cl are arranged with respect to each other and to other fluorines on neighbouring molecules in the fluid. To this end we have calculated the distribution function for the phenyl$_2$-phenyl$_3$ inter-ring torsional angle (as shown in figure 10). In gas phase *ab initio* calculations [10] we saw a four-fold torsional potential with no preference for the fluorines being on either side of the molecule. However, in the liquid phase (figure 10) we see that the peaks at 138° and 222°, which correspond to the fluorines on opposite sides of the molecule, are larger than those at 39° and 320°, which correspond to the fluorines on the same side of the molecule. We therefore see an intramolecular preference for an anti-parallel arrangement of the transverse components of the dipole moment. To examine how fluorines on neighbouring molecules are oriented relative to each other, we calculated distance dependent dipole correlation functions g_1 (as defined by equation 3) for the C-F$_1$ and C-F$_2$ bonds and the cross correlation function involving the angle between

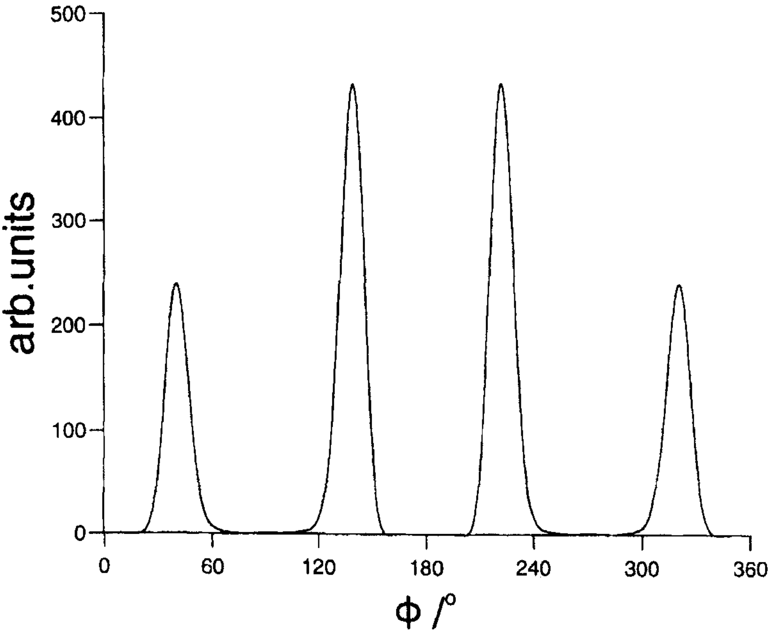

FIGURE 10 The phenyl$_2$-phenyl$_3$ inter-ring torsional angle in the isotropic phase of GGP5Cl (The zero of the torsional angle is defined when two coplanar fluorines are on the same side of the molecule.)

C-F$_1$ and C-F$_2$ bonds, as plotted in figure 11. For all three functions we can detect a sharp positive peak at short distances (≈ 3 Å), a trough at slightly longer distances (≈ 3.5 Å (C-F$_1$), 4 Å (C-F$_2$, C-F$_1$/C-F$_2$)) and a diffuse positive peak at ≈ 6.5 Å. The short distance peak is likely to correspond to configurations C, F and G for C-F$_1$ where two rings lie on top of each other, apart from a small offset in their positions. This is the lowest energy arrangement for two quadrupoles that are constrained parallel to each other. The trough and the diffuse positive peak arise from contributions involving a number of the configurations shown in figure 9.

4 CONCLUSIONS

Together with our previous study on PCH5/PCH5-Cl [9], the calculations presented in this work represent the most accurate all-atom study of mesogenic mol-

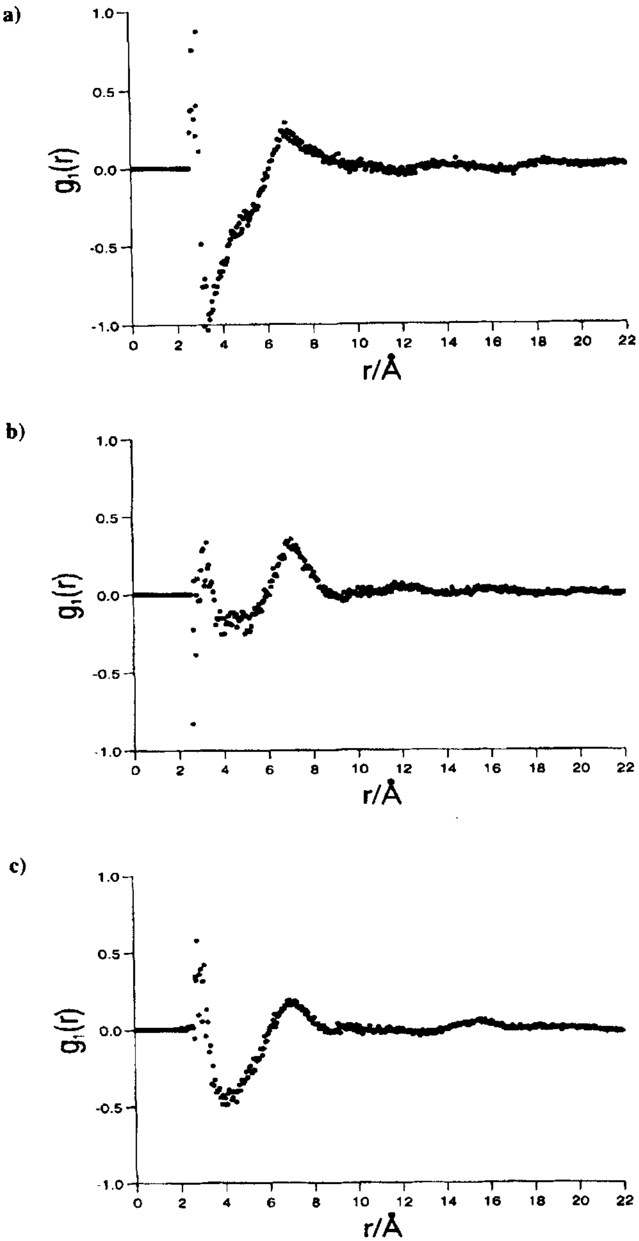

FIGURE 11 Distance dependent dipole correlation functions. a) C-F_1 bond, b) C-F_2 bond, c) cross correlation function for the C-F_1 and C-F_2 bonds

ecules published to date. We have now been able to look at dipole correlation in detail and have been able to reproduce the experimental g_1 result for me5NF.

The picture of dipole correlation in the bulk, viewed in this work, is seen to be extremely complicated. For both molecules, several parallel and anti-parallel dipole dimers can be detected, in addition to some trimers. Extensive analysis of equilibrium MD trajectories has also allowed the identification of the groups that are responsible for the stabilization of these interactions. Interactions between quadupoles on aromatic rings appear to be extremely important in stabilizing particular pair configurations. However, it is evident that small changes in molecular structure could easily influence the balance of which pair configurations are most favoured. It is therefore difficult to use these calculations directly in molecular engineering applications to suggest ways of stabilizing pair configurations that would lead to large effective dipole moments in the bulk.

The work has also examined the relative orientations of two fluorines on separate phenyl rings in the core of GGP5Cl. An intramolecular preference for an anti-parallel arrangement of dipoles is seen. The intermolecular correlation between C-F bond orientations is a complicated one and we see evidence for both parallel and anti-parallel dipole correlation at different distances.

Finally, we note the key importance of electrostatic interactions in determining the local structure of both me5NF and GGP5Cl. Proper handling of long range contributions to the forces and potential using an Ewald sum (or method of equivalent accuracy) is essential to ensure that these interactions are correctly handled in simulations of this type. In addition, it is likely that the absence of any force field terms that are capable of modelling polarization effects in GGP5Cl, leads to inaccuracies in determining the correct balance of anti-parallel and parallel dipole dimers in this highly polarizable material. The absence of these terms is likely to be responsible for the discrepancy between calculated and experimental values of g_1.

Acknowledgements

The authors wish to thank the University of Durham IT service for providing computer time on its parallel Silicon Graphics system, and the UK EPSRC for providing computer time on a Cray T3E. MJC wishes to thank the EPSRC and Merck UK Ltd. for providing a research studentship (1997–2000), and Merck UK Ltd (Southampton) for the gift of a DEC 433 a.u. workstation. The authors wish to thank Dr. M. Bremer and Dr. M. Heckmeier (Merck KGaA, Darmstadt) for valuable discussions and for supplying experimental data for me5NF and GGP5Cl.

References

[1] Wilson, M. R. and Allen, M. P. *Molec. Cryst. Liq. Cryst.* **198**, 465 (1991).
[2] Wilson, M. R. and Allen, M. P. *Liq. Cryst.* **12**, 157 (1992).
[3] Cross, C. W. and Fung, B. *J. Chem. Phys.* **101**, 6839 (1994).
[4] Kolmolkin, A. V., Laaksonen, A., and Maliniak, A. *J. Chem. Phys.* **101**, 4103 (1994).
[5] Hauptmann, S., Mosell, T., Reiling, S., and Brickmann, J. *Chem. Phys.* **208**, 57 (1996).
[6] Yakovenko, S. Y., Muravski, A. A., Kromer, G., and Geiger, A. *Molec. Phys.* **86**, 1099 (1995).
[7] Yakovenko, S. Y., Muravski, A. A., Eikelschulte, F., and Geiger, A. *Liq. Cryst.* **24**, 657 (1998).
[8] McBride, C., Wilson, M. R., and Howard, J. A. K. *Molec. Phys.* **93**, 955 (1998).
[9] Cook, M. J. and Wilson, M. R. *Liq. Cryst.*, accepted for publication (2000).
[10] Cook, M. J. and Wilson, M. R. *Molec. Cryst. Liq. Cryst.*, in press (2000).
[11] Ryckaert, J. P., Ciccotti, G., and Berendsen, H. J. C. *J. Chem. Phys.* **23**, 327 (1977).
[12] Forester, T. R. and Smith, W. *DL_POLY_2.11*. DL_POLY is a package of molecular simulation routines written by W. Smith and T. R. Forester, copyright The Council for the Central Laboratory of the Research Councils, Daresbury Laboratory at Daresbury, Nr. Warrington (1996).
[13] Dunmur, D. A. and Wilson, M. R. *J. Chem. Soc. Faraday Trans. 2* **84**, 1109 (1988).
[14] Bremer, M. *personal communication.* (Work carried out at Merck KGaA, Darmstadt).
[15] Veerman, J. A. C. and Frenkel, D. *Phys. Rev. A* **41**, 3237 (1990).
[16] Wilson, M. R. PhD thesis, University of Sheffield, (1988).
[17] Toriyama, K. and Dunmur, D. A. *Molec. Cryst. Liq. Cryst.* **139**, 123–142 (1986).
[18] Dunmur, D. A. and Toriyama, K. *Liq. Cryst.* **1**, 169 (1986).
[19] Dunmur, D. A. and Toriyama, K. *Molec. Cryst. Liq. Cryst.* **264**, 131 (1995).